

# In Situ Particle Behavior of Cast Iron Powder by Suspension Plasma Spraying

C. Tekmen, K. Iwata, Y. Tsunekawa, and M. Okumiya

(Submitted April 21, 2009; in revised form October 7, 2009)

**An important issue for atmospheric plasma sprayed metal coatings is the oxidation involved during processing that significantly affects its phase composition and microstructure and thus the overall coating properties. In this study, suspension thermal spraying was used to manufacture cast iron coatings with high amounts of graphite carbon as solid-lubricant, because graphite structure is considerably diminished in molten droplets of the spray material due to the dissolution into molten iron and/or the oxidation. Additional graphite formation based on the soot reaction of liquid hydrocarbon was observed. Oxidation strongly affects the soot reaction during suspension thermal spraying. Therefore, setting-up of a shroud around the plasma plume is quite effective to prevent the oxidation of hydrocarbon.**

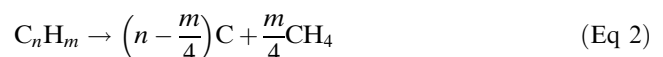
**Keywords** cast iron, graphite, hydrocarbon, plasma spraying, shroud, soot, suspension

## 1. Introduction

In automobile industry, particularly the surface treatment of cylinder bore in aluminum engine blocks remains a key challenge in order to improve the poor tribological properties of aluminum. Among the various surface treatment methods including etching, infiltration, electroplating, aluminum wet liners and laser etching, plasma spraying has proved itself as an alternative method by achieving 4% reduction in fuel consumption and is continuously gaining importance (Ref 1). However, the average cost per unit of plasma sprayed bore compared to cast iron liner is still high; therefore, new approaches are needed to reduce the cost without incurring yet improving the performance. Plasma sprayed cast iron coatings containing graphite as solid lubricant are potential candidates to replace traditional steel or ferrous coatings for the surface modification of aluminum, due to the superior wear resistance arising from the self-lubricating effect of

graphite and relatively low cost of cast iron powder (Ref 2). It has been shown that the wear resistance of cast iron increases with the increase in graphite content (Ref 3). However, the graphite content in cast iron coating strongly depends on the spray parameters as well as the powder properties (size and composition) and might be altered due to the oxidation and/or dissolution during plasma spraying (Ref 4, 5). Moreover, the improper selection of spray parameters may lead to form carbides instead of graphite in cast iron coatings. Recently, it has been demonstrated that the amount of graphite carbon can be controlled by in-flight particle diagnostic such that by preventing the in-flight oxidation of graphite (Ref 6). Therefore, in view of improving the tribological properties of cast iron coatings, there is a need to promote the graphite structure. Several methods and factors including pre-annealing of cast iron powder, post-annealing of the coating, adding alloying elements, in-process graphitization, substrate preheating, powder properties, and chamber pressure have been investigated to improve the graphite structure in cast iron coatings (Ref 7-10).

In this study, in order to increase the graphite content, different hydrocarbons as liquid suspension (hexane and toluene) and as gas precursor (methane) were introduced into the plasma plume. The increase in graphite content is expected to occur through the decomposition of methane (Eq 1) and pyrolysis of liquid hydrocarbon (Eq 2), in the high-temperature plasma jet, according to the following in situ reactions (at ambient pressure):



Although several liquid and gas precursors have been investigated to deposit thin and dense layers (Ref 11), this paper makes the first attempt in the respect of improving the graphite content in cast iron coatings by using liquid hydrocarbons.

This article is an invited paper selected from presentations at the 2009 International Thermal Spray Conference and has been expanded from the original presentation. It is simultaneously published in *Expanding Thermal Spray Performance to New Markets and Applications: Proceedings of the 2009 International Thermal Spray Conference*, Las Vegas, Nevada, USA, May 4-7, 2009, Basil R. Marple, Margaret M. Hyland, Yuk-Chiu Lau, Chang-Jiu Li, Rogerio S. Lima, and Ghislain Montavon, Ed., ASM International, Materials Park, OH, 2009.

**C. Tekmen, K. Iwata, Y. Tsunekawa, and M. Okumiya**, Toyota Technological Institute, Materials Processing Laboratory, 2-12-1 Hisakata, Tempaku, 468-8511 Nagoya, Japan. Contact e-mail: ctekmen@gmail.com.

## 2. Experimental Procedure

### 2.1 Powder Preparation

Fe-4C-3.8Si-4Al (in wt.%) powder manufactured by water atomization process with a particle size range of 32-62  $\mu\text{m}$  was used as starting material. Silicon and aluminum were introduced as anti-oxidizer and strong graphitizer by reducing supercooling through providing an adequate number of suitable nuclei for graphite growth and minimizing the tendency to form carbides (Ref 12). In order to increase the graphite content, cast iron powder was pre-annealed at 900  $^{\circ}\text{C}$  for 1 h at low pressure (15 Pa) and slowly cooled (in furnace) to room temperature. XRD patterns (in as-received and annealed conditions) and morphology of the cast iron powder are given in Fig. 1. The strong iron silicon carbide and aluminum iron carbide

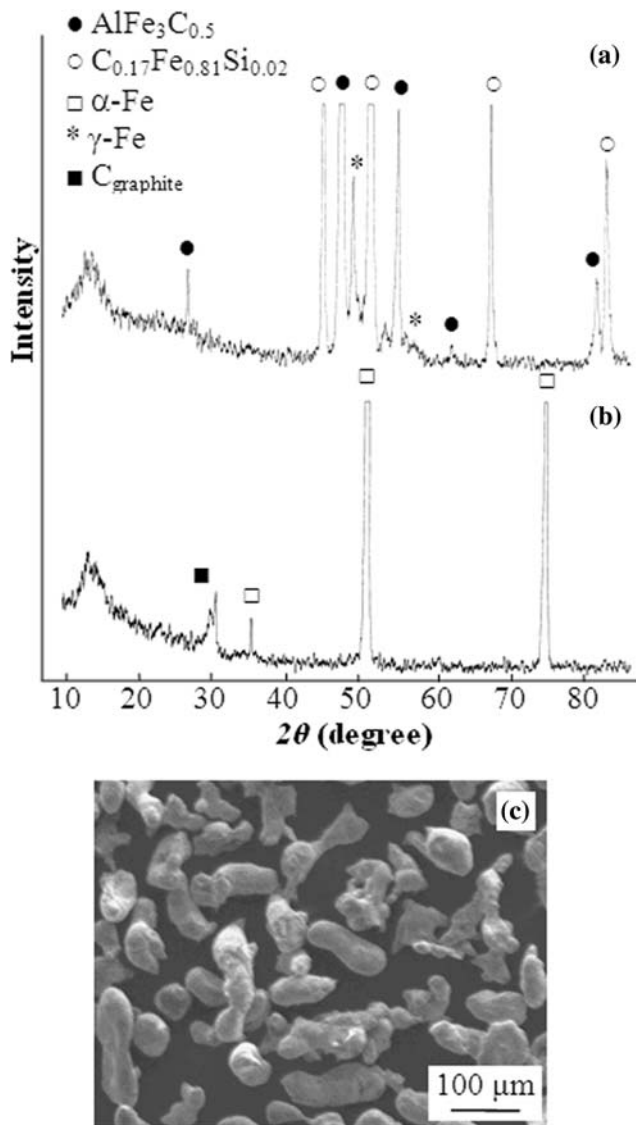


**Fig. 1** XRD patterns of cast iron powder: (a) as-received, (b) annealed, and (c) powder morphology

peaks observed in as-received condition are due to the rapid solidification of the cast iron powder during the water atomization process which discourages the nucleation of graphite and promotes the formation of thermodynamically metastable iron carbide. It is clear that after the annealing process these peaks disappear and are replaced by  $\alpha\text{-Fe}$  and graphite peaks. As a result, about 3.8 wt.% of graphite is precipitated in cast iron powder by owing a high ratio (0.95) of graphite carbon (GC) to total carbon (TC).

### 2.2 Plasma Spraying

Grit-blasted ( $\text{Al}_2\text{O}_3$ , 425-500  $\mu\text{m}$  particle size) Al-11.2Si-2.74Cu (in wt.%) die cast aluminum (ADC12) plate ( $30 \times 30 \times 5 \text{ mm}^3$ ) was used as substrate. Mean surface roughness ( $R_a$ ) of the substrate after grit-blasting was measured as  $5.05 \pm 0.77 \mu\text{m}$  by using a surface roughness tester (Mitutoyo, SV-400). Atmospheric plasma spraying (APS) of the coatings was carried out using Sulzer Metco (Wohlen, Switzerland) 9 MB plasma gun under conditions given in Table 1. Powders were injected perpendicularly to the plasma jet axis through a 2 mm inner-diameter (ID) port located 3 mm downstream of the nozzle exit.

### 2.3 Injection of Liquid Hydrocarbon

As illustrated in Fig. 2, hexane ( $\text{C}_6\text{H}_{14}$ ) and toluene ( $\text{C}_7\text{H}_8$ ) were introduced into the plasma flame by using a syringe pump with a 0.25 mm ID nozzle placed 6 mm apart from the downstream gun exit. The liquid feeding rate was 6  $\text{cm}^3/\text{s}$ . Besides, methane ( $\text{CH}_4$ ) was introduced as a carrier gas. Also, a stainless steel cube-shaped shroud ( $10 \times 10 \times 10 \text{ cm}$ ) was used in order to investigate the oxidation behavior of liquid hydrocarbons during plasma spraying. Coating combinations investigated in this study are given in Table 2.

### 2.4 Characterization

Coated samples were characterized by means of x-ray diffractometer (XRD) with  $\text{CoK}\alpha$  radiation, scanning electron microscope (SEM), optical microscope and electron probe microanalysis (EPMA). GC and TC contents in cast iron coatings were determined by an infrared absorption method using the peeled off coatings from the

**Table 1** Plasma spray parameters

Parameter	Injection	
	Using methane as carrier gas	hexane/toluene as liquid hydrocarbon
Primary gas flow rate, L/min: Ar	40	40
Secondary gas flow rate, L/min: $\text{H}_2$	2	2
Current, A	375	400
Voltage, V	44	50
Stand-off distance, mm	150	100
Nozzle inner diameter, mm	7.8	5.6
Carrier gas flow rate, L/min	6 (methane)	6 (argon)

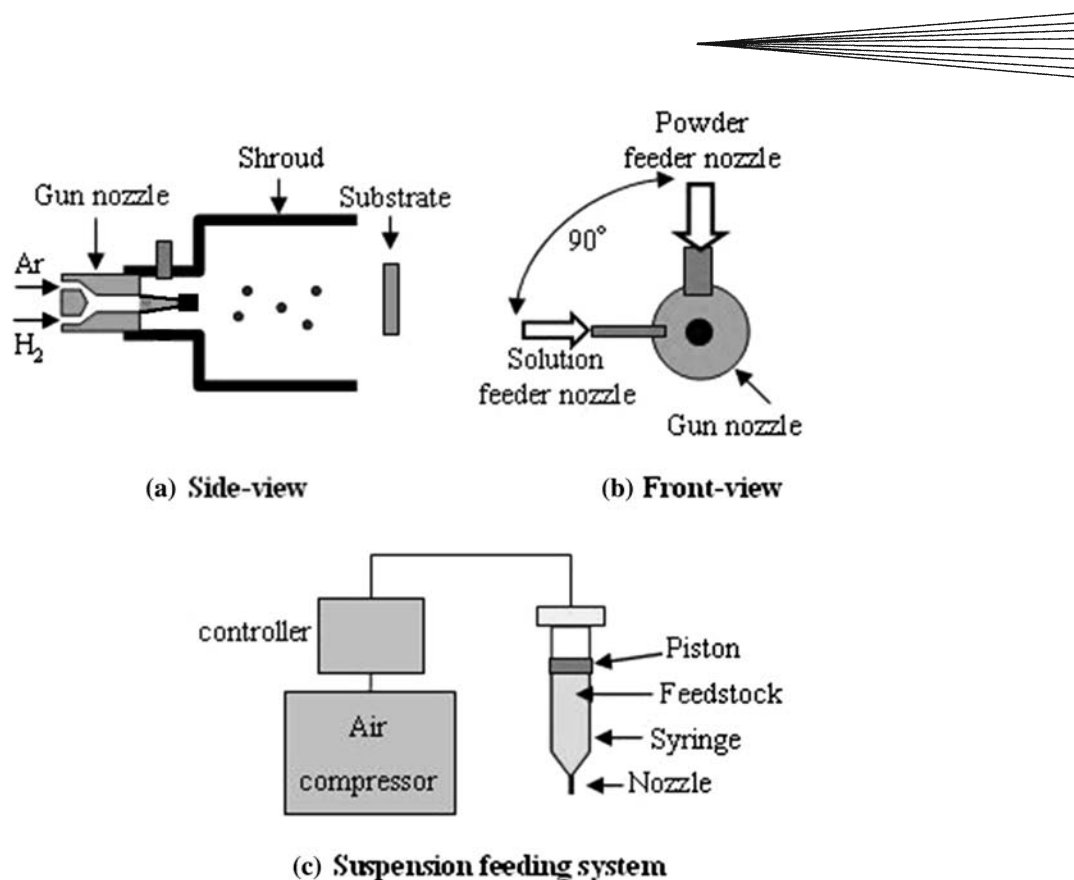


Fig. 2 Schematic illustration of the suspension feeding system and shroud design

Table 2 Coating combinations

Condition	Powder	
	Pure iron	Cast iron
Argon as carrier gas (as-sprayed)	X	X
Methane as carrier gas	X	
Hexane injection	X	
Toluene injection	X	X
Hexane injection and using a shroud	X	
Toluene injection and using a shroud	X	X

substrate. Also, in order to accurately determine and specify the amount and structure of the carbon resulting from methane, hexane and toluene addition, as-received pure (>99%) iron powder and only liquid hydrocarbon were sprayed under same spray conditions.

### 3. Results and Discussion

#### 3.1 Effect of Methane

Methane was introduced into the plasma flame as a carrier gas in order to decrease the in-flight particle temperature of cast iron powder and prevent the oxidation and dissolution of graphite as well as to provide additional free carbon through the endothermic decomposition of methane (Eq 1). However, based on EPMA and chemical

analyses of the coatings sprayed with pure iron powder by using argon and methane as a carrier gas, it can be said that the effect of methane on the total carbon amount is insignificant (Fig. 3). The reason could be that methane rapidly dissociated into  $\text{CH}_x$  and  $\text{H}_{(4-x)}$  through the charge transfer from Ar ions present in the plasma.  $\text{CH}_4$  does not form stable carbon species to precipitate in the molten droplet and/or after impinged onto the substrate (Ref 11). Therefore, introducing methane into the plasma plume is not an effective method to precipitate higher amounts of graphite. A more detailed discussion on the influence of methane on in-flight particle behavior of cast iron powder by atmospheric plasma spraying can be found in Ref 13.

#### 3.2 Soot Formation

XRD analyses of the carbon (also called sprayed soot) in the sample sprayed with only toluene injection were performed by comparing with as-received carbon black and graphite powder (Fig. 4). Results indicate that the structure of the carbon formed according to Eq 2 is very similar to carbon black. In other words, the incomplete combustion or pyrolysis of toluene in the plasma plume results in the formation of soot carbon (SC). Soot particles are described as small crystallites (quasi-spherical particles) ranging from about 10 to 500 nm in size and having a turbostratic graphitic structure where the crystallites are randomly oriented and connected to one another by single planes or by amorphous carbon (Ref 14). It is believed that soot particles form in three stages. The first stage

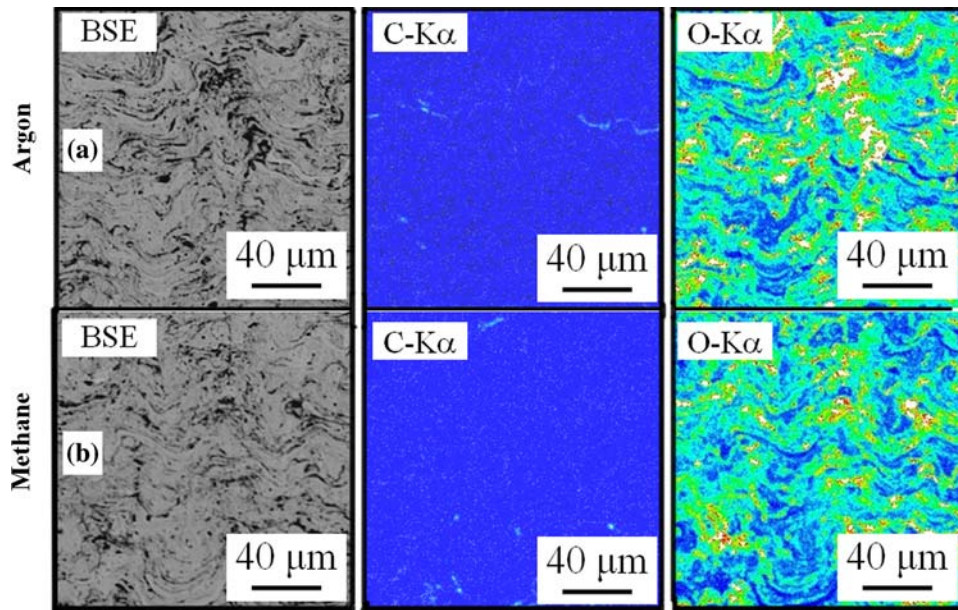


**Fig. 3** Back-scattered electron (BSE) and x-ray images of the coatings sprayed with pure iron powder by using (a) argon and (b) methane as a carrier gas. O-K $\alpha$ , oxygen; C-K $\alpha$ , carbon

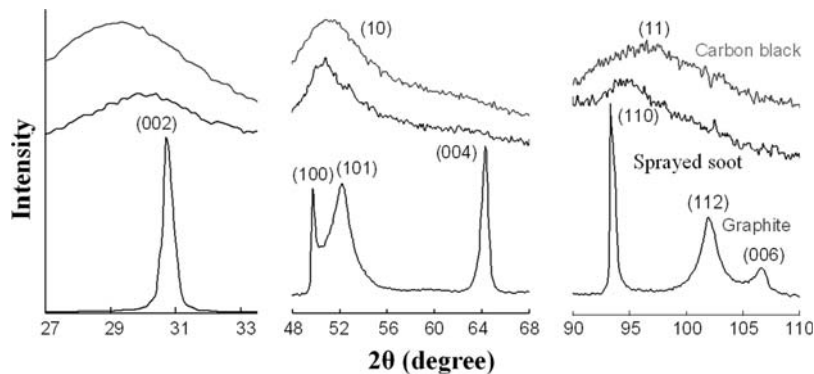


**Fig. 4** XRD patterns of carbon black, sprayed soot, and graphite

involves the reactions between hydrocarbon species and eventually condenses out of the vapor phase to form nuclei. In the second stage, nuclei coalescence and surface deposition processes occur. And finally in the last stage, relatively large spheroidal particles join together to form long chains (Ref 15). In plasma spraying, the transition of these stages assumed to be completed in about  $10^{-3}$  s.

### 3.3 Effect of Toluene and Hexane

Chemical analyses were performed on hexane and toluene injected pure iron coatings with and without using a shroud in order to precisely determine the total carbon and soot carbon content (Fig. 5). Although the total carbon content is about 0.38 wt.% in the coatings sprayed by injecting hexane or toluene, the increase is worthwhile if we consider that the initial carbon content in pure iron

powder is  $<0.01$  wt.%. In the case of using cast iron powder, in addition to soot carbon the coating contains also graphite carbon. Since no graphite peak was observed in sprayed toluene (Fig. 4), the difference in graphite carbon content in as-sprayed and toluene injected coatings corresponds to the amount of soot carbon (Fig. 6). Graphite and soot carbon content in toluene injected cast iron coating is found to be about 2.9 and 0.8 wt.%, respectively. The fraction of the sum of graphite and soot carbon to total carbon content is about 76%. Herein, the difference ( $\Delta C$ ) between total and graphite carbon corresponds to the carbon dissolved into iron matrix. The dissolution of carbon from graphite is thought to be occurring through the dissociation of carbon atoms from its crystal site in the graphite into the carbon/melt interface and subsequently the mass transfer of carbon atoms into the molten iron (Ref 16).

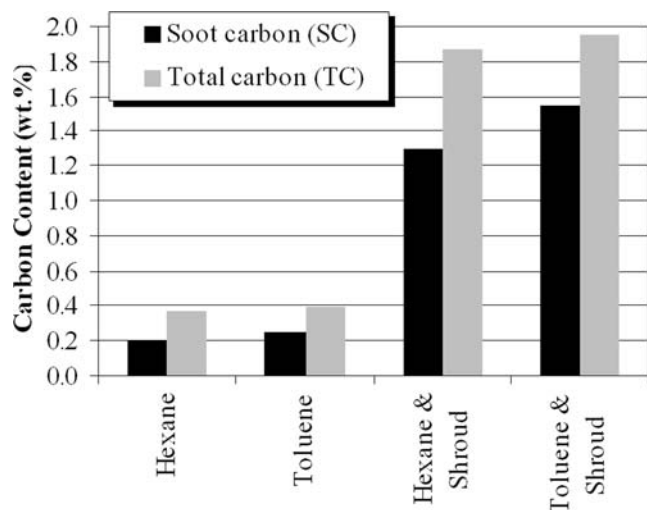


**Fig. 5** Total carbon (TC) and soot carbon (SC) content of pure iron coatings sprayed with injecting hexane and toluene with and without using a shroud

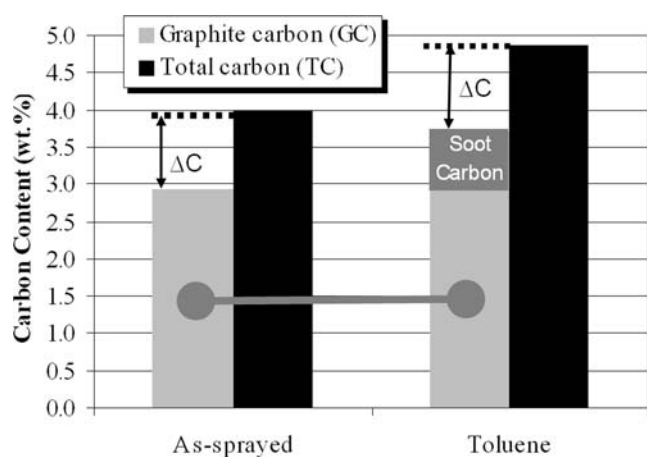


**Fig. 6** Total carbon (TC), graphite carbon (GC), and soot carbon (SC) contents of cast iron coatings sprayed with toluene injection

### 3.4 Effect of Shroud

In the case of using a shroud, the increase in carbon content is remarkable. For toluene injected coatings, when using a shroud the total carbon content increases by 428% which corresponds to a value of 1.95 wt.%, and the increase in soot carbon content is about 525% by achieving a value of 1.55 wt.% (Fig. 5). The effect of toluene injection and shroud use on the coating structure and the amount of carbon and oxygen were investigated by means of EPMA analyses (Fig. 7). Pure iron coating exhibits a wavy oxide at the interfaces between layered splats, whereas coatings produced with toluene injection have very weak O-K $\alpha$  intensity, which might be explained by the depletion of present oxygen through the combustion

of toluene. Toluene is known as a flammable liquid substance at room temperature, so it is ready to oxidize instead of soot formation through the pyrolysis reaction in atmospheric plasma spraying. Besides, it is obvious that using a shroud remarkably increases the amount of soot carbon by reducing the amount of oxygen and, hence, induces the pyrolysis reaction of toluene. In other words, in situ soot formation is predominant compared with oxidation. Consequently, when combined with the use of shroud, liquid hydrocarbon injection into the plasma plume permits not only to prevent in-flight particle oxidation, but also to form additional soot carbon structure in iron coatings. This method can be widely applied to other types of spray coatings as well.

### 3.5 Microstructure

XRD analysis of toluene injected cast iron coatings sprayed with using a shroud shows that the coating is composed of  $\alpha$ -Fe,  $\gamma$ -Fe,  $C_{0.17}Fe_{0.81}Si_{0.02}$ , and  $C_{\text{graphite}}$  (Fig. 8). Rapid solidification of the coating sprayed with pre-annealed powder leads to form the same phases as observed in as-received powder (Fig. 1a), which is also rapidly solidified. It can be said that the solidification rate is high enough to form carbide but as well slow enough to retain metastable  $\gamma$ -Fe in the structure. Besides the effect of creating active nucleus for the precipitation of graphite, it is expected that alloying cast iron powder with silicon and aluminum lowers the thermal conductivity, thus decreasing the solidification rate during plasma spraying (Ref 17, 18). Also, it has been reported that an increase in wear resistance has been observed by plasma spraying cast iron powder with high Si and Al content (Ref 19).

In spite of the self-lubricating effect of graphite, this element may deteriorate the adhesion between the substrate and coating. Therefore, it is important to obtain a graphite-like structure only close to the surface of the coating. Subsequently injecting the hydrocarbon into the plasma flame makes possible to achieve such a coating structure as demonstrated in Fig. 9, where soot carbon (black color regions) in cast iron coating can be easily distinguished. As a result, it can be said that a coating such that exhibiting a graphite-like structure close to the surface may improve the tribological properties of cast iron coatings.

### 3.6 Graphitization

As well known, the wear rate depends strongly on the graphitization degree ( $P_1$ ), which is the probability to get a pair of aromatic layers in the graphite order (Ref 20). In this study, the degree of graphitization of sprayed soot, carbon black and synthesized graphite was calculated through the intensity ratio of the (002) diffraction peak of the specimen relative to a defined graphite standard and is found to be 0.02, 0.04, and 0.79, respectively. This result indicates that the degree of graphitization of the sprayed soot is relatively low to improve the wear properties of cast iron coatings. However, as seen from Fig. 10, it is possible to increase the graphitization degree by

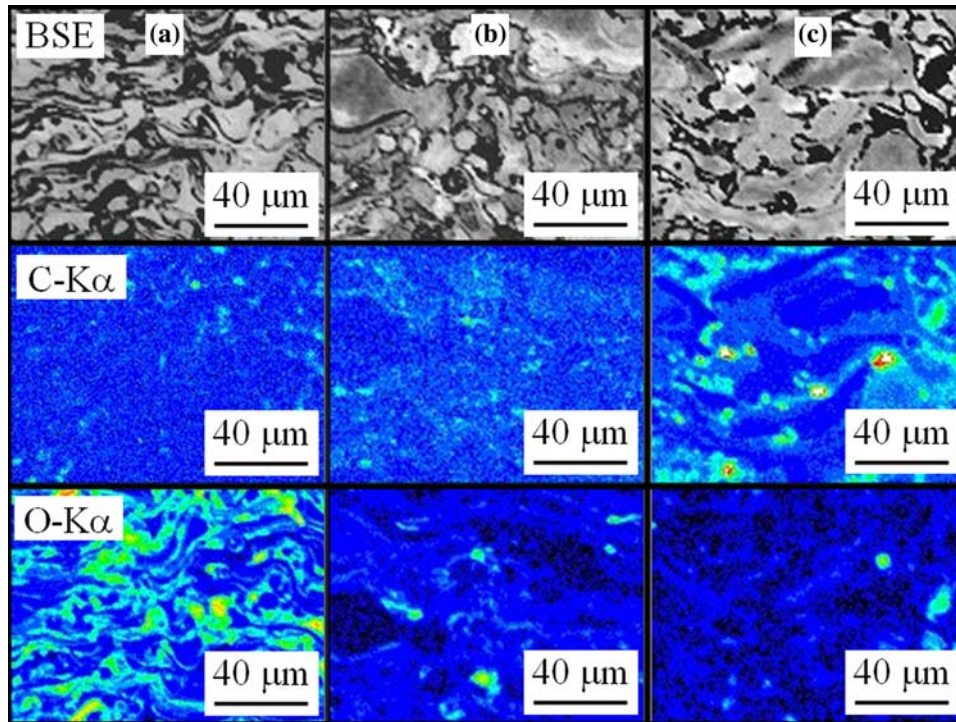


**Fig. 7** BSE and x-ray images of pure iron coating: (a) as-sprayed, (b) with toluene injection, and (c) with toluene injection and using a shroud. O-K $\alpha$ , oxygen; C-K $\alpha$ , carbon

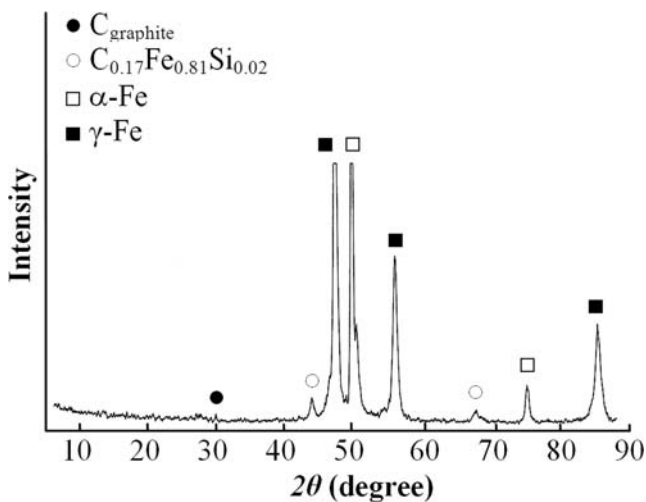


**Fig. 8** XRD pattern of toluene injected cast iron coating with using a shroud

transforming soot into graphite by applying a post-annealing process at 1150 °C for 2 h in nitrogen atmosphere. It has been reported that upon heating the initial nanostructured quasi-spherical soot particle templates grow as a “sphere” with many flat sides, i.e. polygonal in nature (Ref 21). Therefore, it can be expected that using graphitized soot as a solid lubricant may improve the wear resistance of cast iron coatings.

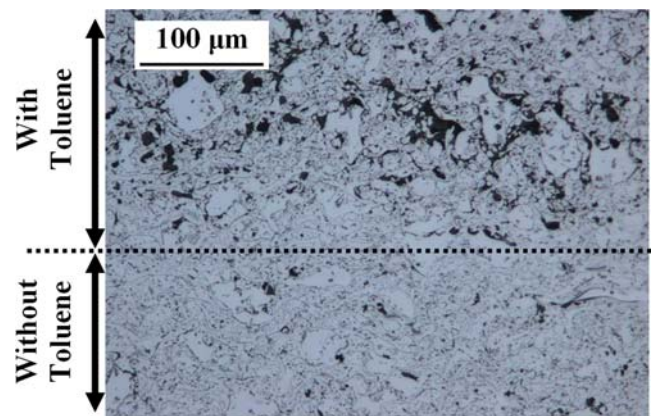


**Fig. 9** Cross-sectional microstructure of cast iron coating where toluene is subsequently injected

It is of interest to note that the graphitization of soot occurred at relatively low temperature, because it is generally accepted that graphitization starts above 2000 °C and the interlayer spacing between neighboring layers ( $d_{002}$ ) decreases and approaches the value of graphite between 2200 and 2300 °C (Ref 22, 23). Also, it is clear that pure iron powder is oxidized by forming FeO, Fe<sub>2</sub>O<sub>3</sub>, and Fe<sub>3</sub>O<sub>4</sub> iron oxides during plasma spraying (in-flight) or after deposition onto the substrate which also explains the regions with relatively high intensity of O-K $\alpha$  observed in pure iron coatings sprayed without toluene

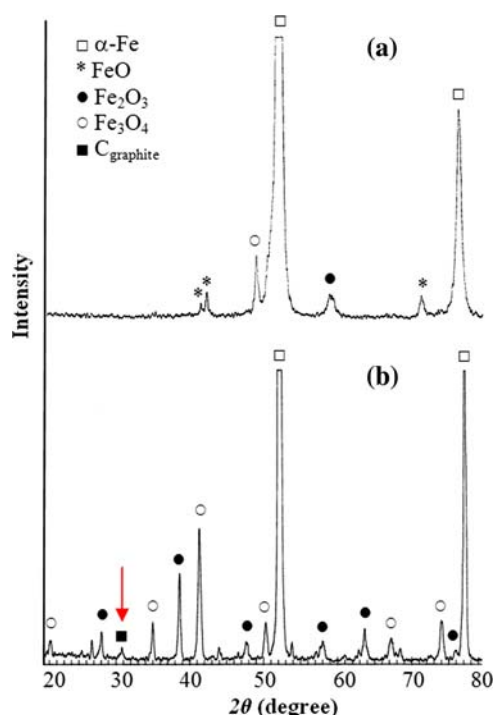


**Fig. 10** XRD pattern of toluene injected pure iron coating (a) before and (b) after annealing

injection (Fig. 7). These iron oxides might act as catalysts and lead the graphitization of soot occurring at relatively low temperature (so-called catalytic graphitization). A detailed overview of using compounds as a catalyst in graphitization can be found in Ref 24.

## 4. Conclusions

In this study, it was demonstrated that cast iron coatings containing soot carbon can be sprayed by injecting liquid hydrocarbon such as hexane or toluene into the flame. Besides forming additional soot carbon structure, liquid hydrocarbon injection remarkably prevents the in-flight particle oxidation. Also, it has been observed that using a shroud during plasma spraying strongly increases the amount of soot carbon in cast iron coatings which can be transformed into graphite by applying a post-annealing process. This method offers new perspectives in the field of wear resistant applications by promoting a graphite-like structure in cast iron coatings.

## References

1. G. Barbezat, Advanced Thermal Spray Technology and Coating for Lightweight Engine Blocks for the Automotive Industry, *Surf. Coat. Technol.*, 2005, **200**, p 1990-1993
2. I. Ozdemir, Y. Tsunekawa, M. Okumiya, and T. Ueno, Graphitization Potential of Cast Iron Powder in Atmospheric Plasma Spray Conditions, *Mater. Trans.*, 2006, **47**(7), p 1710-1716
3. E. Takeuchi, M. Matsunaga, T. Nakagawa, F.-S. Dai, and H.-Y. Ra, Friction and Wear of Sintered Cast Iron Products, *Wear*, 1982, **75**(2), p 303-312
4. I. Ozdemir, T. Ueno, Y. Tsunekawa, and M. Okumiya, Cast Iron Coatings Containing Graphite Structure by Atmospheric Plasma Spraying, *Thermal Spray: Advances in Technology and Application*, May 10-12, 2004 (Osaka, Japan), ASM International, 2004, p 298-303
5. Y. Tsunekawa, I. Ozdemir, T. Ueno, and M. Okumiya, Change in Graphite Structure of Cast Iron Coatings through the Process of Plasma Spraying, *Surf. Modif. Technol.*, 2006, **XVIII**, p 3-9
6. K. Iwata, C. Tekmen, Y. Tsunekawa, and M. Okumiya, Graphite Structure in Coatings by Plasma Spraying with Iron Powder and Suspension, *Asian Thermal Spray*, Nov 6-8, 2008 (Singapore), CD-ROM
7. Y. Tsunekawa, I. Ozdemir, and M. Okumiya, Plasma Sprayed Cast Iron Coatings Containing Solid Lubricant Graphite and h-BN Structure, *J. Therm. Spray Technol.*, 2006, **15**(2), p 239-245
8. M.F. Morks, Y. Tsunekawa, M. Okumiya, and M.A. Shoeib, Splat Morphology and Microstructure of Plasma Sprayed Cast Iron with Different Preheat Substrate Temperatures, *J. Therm. Spray Technol.*, 2002, **11**(2), p 226-232
9. M.F. Morks, Y. Tsunekawa, M. Okumiya, and M.A. Shoeib, Splat Microstructure of Plasma Sprayed Cast Iron with Different Chamber Pressures, *J. Therm. Spray Technol.*, 2003, **12**(2), p 282-289
10. M.F. Morks, Y. Tsunekawa, M. Okumiya, and M.A. Shoeib, Microstructure of Plasma-Sprayed Cast Iron Splats with Different Particle Sizes, *Mater. Trans.*, 2003, **44**(4), p 743-748
11. J.L. Dorier, Ph. Guittienne, Ch. Hollenstein, M. Gindrat, and A. Refke, Mechanism of Films and Coatings Formation from Gaseous and Liquid Precursors with Low Pressure Plasma Spray Equipment, *Surf. Coat. Technol.*, 2008, **203**(15), p 2125-2130
12. J. Lampman and A. Peters, *Ferroalloys and Other Additives to Liquid Iron and Steel*, STP 739, Special Technical Publications, ASTM, 1981, p 125-143
13. C. Tekmen, K. Iwata, Y. Tsunekawa, and M. Okumiya, Influence of Methane and Carbon Dioxide on In-Flight Particle Behavior of Cast Iron Powder by Atmospheric Plasma Spraying, *Mater. Lett.*, 2009, **63**(28), p 2439-2441
14. B. Dippel, H. Jander, and J. Heintzenberg, NIR FT Raman Spectroscopic Study of Flame Soot, *Phys. Chem. Chem. Phys.*, 1999, **1**, p 4707-4712
15. J.B. Donnet, R.C. Bansal, and M.J. Wang, Ed., *Carbon Black*, 2nd ed., CRC Press, New York, 1993
16. S.T. Cham, R. Sakurovs, H. Sun, and V. Sahajwalla, Influence of Temperature on Carbon Dissolution of Cokes in Molten Iron, *ISIJ Int.*, 2006, **46**(5), p 652-659
17. M.F. Morks, Y. Tsunekawa, and M. Okumiya, Characterization and Properties of Splats Sprayed with Different Cast Iron Powders, *Mater. Lett.*, 2004, **58**, p 2481-2485
18. M.F. Morks, Y. Tsunekawa, N.F. Fahim, and M. Okumiya, Microstructure and Friction Properties of Plasma Sprayed Al-Si Alloyed Cast Iron Coatings, *Mater. Chem. Phys.*, 2006, **96**, p 170-175
19. M.F. Morks, M.A. Shoeib, Y. Tsunekawa, and M. Okumiya, Effect of Powder Composition on the Microstructure and Wear Properties of Sprayed Cast Iron Coatings, *Thermal Spray: Advancing the Science and Applying Technology*, May 5-8, 2003 (Florida), ASM International, 2003, p 317-322
20. P.A. Grattan and J.K. Lancaster, Abrasion by Lamellar Solid Lubricants, *Wear*, 1967, **10**, p 453-468
21. K.W. Street, M. Marchetti, R.L. Vander Wal, and A.J. Tomasek, Evaluation of the Tribological Behavior of Nano-Onions in Krytox 143AB, *Tribol. Lett.*, 2004, **16**(1-2), p 143-149
22. P.A. Thrower and L.R. Radovic, *Chemistry and Physics of Carbon*, Vol 26, CRC Press, Boca Raton, 1999, p 135
23. C.R. Houska and B.E. Warren, X-Ray Study of the Graphitization of Carbon Black, *J. Appl. Phys.*, 1954, **25**(12), p 1503-1509
24. A. Oya and H. Marsh, Review Phenomena of Catalytic Graphitization, *J. Mater. Sci.*, 1982, **17**, p 309-322